

Investigation of the Relationship between ELM Energy Loss and Perturbed Electron Transport on NSTX

K. Tritz¹, M. Bell², R. Bell², L. Delgado-Aparicio¹, M. Finkenthal¹, S. Kaye², B. LeBlanc², R. Maingi³, J. Menard², D. Stutman¹

¹Johns Hopkins University, Baltimore, MD, USA

²Princeton Plasma Physics Laboratory, Princeton, NJ, USA

³Oak Ridge National Laboratory, Oak Ridge, TN, USA

Motivation

The National Spherical Torus Experiment (NSTX) experiences a range of edge localized mode (ELM) behavior during different regimes of H-mode operation^{1,2}. While many of the ELM types demonstrate similar characteristics to those observed in other devices, at low collisionality ($\nu_*^e \leq 1$) large Type I ELMs can occur causing a significant reduction in plasma total stored energy, $\Delta W_{tot}/W_{tot} \sim 15\text{-}30\%$. This loss is primarily due to a reduction of electron thermal energy, evidenced by a global drop in the electron temperature profile as measured by the multipoint Thomson scattering system (MPTS), while the core electron density profile is relatively stable over the same ELM with a loss of the “ears” on the density profile as the ELM expels impurities at the edge (fig. 1). The constancy of the core density profile indicates

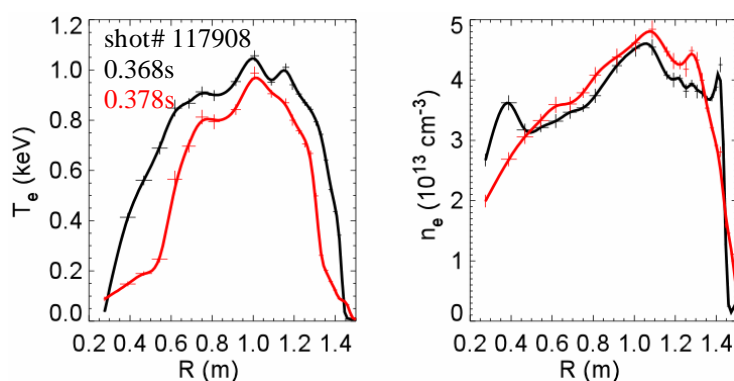


Fig. 1: Electron temperature and density profiles from MPTS before (black) and after (red) large Type I ELM

that, while the ELM itself causes a mixture of convective (particle) and conductive (thermal) losses at the edge, the resultant global perturbation is primarily a conductive loss of energy. Because this stored energy loss is mainly through

the electron thermal channel, a relationship between the electron thermal transport, and more specifically, the perturbed electron thermal transport, χ_e^{pert} , and the severity of the ELM as measured by $\Delta W_{tot}/W_{tot}$ is suggested. Though the MPTS system can provide detailed profile

“snapshots” before, during, and after an ELM, the Ultra Soft X-ray (USXR) system can provide continuous, spatially resolved measurements that are also sensitive to T_e and n_e with time resolution of a few microseconds³.

Experimental Results

The time history of a typical large Type I ELM perturbation on the USXR emission profile is shown in fig. 2. As the global n_e profile is roughly constant, the relative USXR intensity is

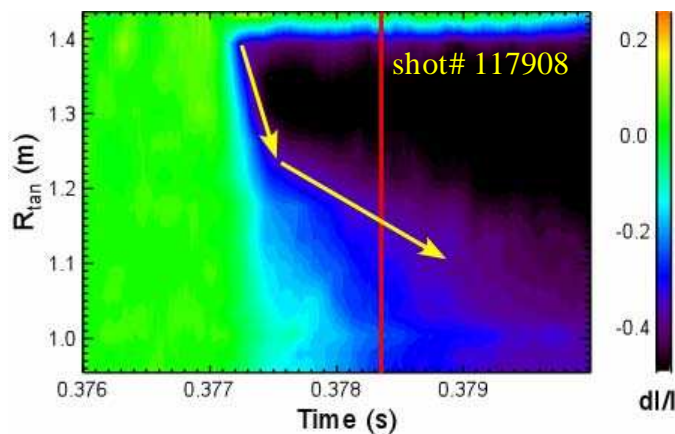


Fig. 2: Relative USXR intensity during Type I ELM cold pulse showing regions of fast and slow propagation (MPTS point time in red).

proportional to the T_e perturbation, and can be used to track the propagation of the induced cold pulse as it travels from the edge to the core of the plasma. The characteristics of the cold pulse perturbations in this plasma regime are consistent, and involve an initial prompt drop in the T_e profile at the plasma boundary followed by a cold pulse that moves

radially inward. The cold pulse progresses rapidly through the outer half of the plasma volume, then slows significantly near the plasma mid-radius before finally reaching the magnetic axis at $R_{axis}=1.03\text{m}$. The total time scale for these perturbations is $\sim 1\text{-}5\text{ms}$, though the initial phase of the rapid propagation lasts only a few hundred microseconds. The MPTS profile snapshot of the perturbed electron temperature, shown previously in fig. 1, corresponds well to the radial extent of the perturbation measured by the USXR system, with the cold pulse front at $\sim 1.15\text{m}$ near the time of the second Thomson Scattering measurement.

Perturbation Analysis

To investigate the relationship between the magnitude of the energy loss from the ELM and the perturbed electron thermal transport in the NSTX plasma, a sawtooth heat pulse model

was used to calculate χ_e^{pert} from the measurement of the radial position of the propagating cold front as a function of the time-to-peak⁴,

$$\chi_e^{pert} \approx \frac{\Delta r_{eff}^2}{8\Delta t_{peak}} \quad (1)$$

where r_{eff}^2 is the minor radius based on the effective area of the flux surface. For these highly shaped NSTX plasmas with a significant Shafranov shift, $\Delta r_{eff}^2 \approx 4\Delta r^2$, where Δr_{eff} and Δr are, respectively, the effective and real space radial extent of the cold pulse. Using Eq. 1, a perturbed electron thermal transport coefficient can be calculated for a variety of ELMs.

Applying the sawtooth model to the USXR cold pulse data from the ELM shown in Fig. 2, it is apparent that two distinct regions of perturbed electron thermal transport exist. A high transport region, $\chi_e^{pert} \sim 100\text{-}200 \text{ m}^2/\text{s}$, is located at $r/a > 0.5$, which also corresponds to the region of high T_e gradient. In the plasma core, χ_e^{pert} is rather flat at $\sim 10\text{-}20 \text{ m}^2/\text{s}$. This region of reduced perturbed transport corresponds to a lower T_e gradient, as shown in Fig. 3. Given the correlation between the high levels of perturbed electron thermal transport and the region

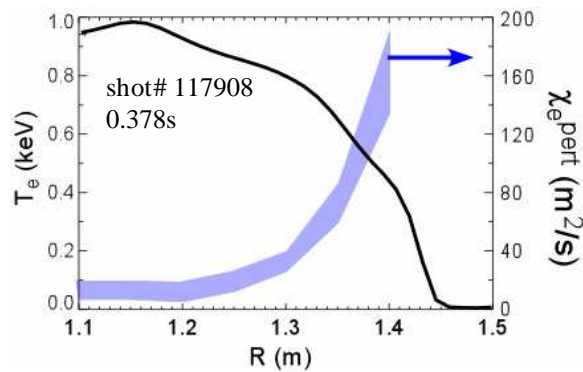


Fig. 3: Calculated perturbed electron thermal transport during large ELM

of high T_e gradient, it is perhaps natural to invoke the idea of a “critical gradient” in T_e , by which any attempt to further steepen the T_e profile is met by a dramatic increase in transport. Also of note, the shape of the χ_e^{pert} profile is different from the steady state χ_e which is highest in the region of flat T_e , as might be expected.

Discussion

Pellet perturbation studies on NSTX have indicated the possible existence of a critical gradient for similar high power discharges on NSTX, but lower power H-mode discharges and L-mode discharges do not exhibit the same profile stiffness found in discharges at or near the critical gradient⁵. Also, perturbations caused by smaller Type I ELMs in different plasma

regimes show markedly different cold pulse behavior (Fig. 4). The cold pulse moves more slowly at the edge, accelerating as it reaches the plasma core with a propagation time of

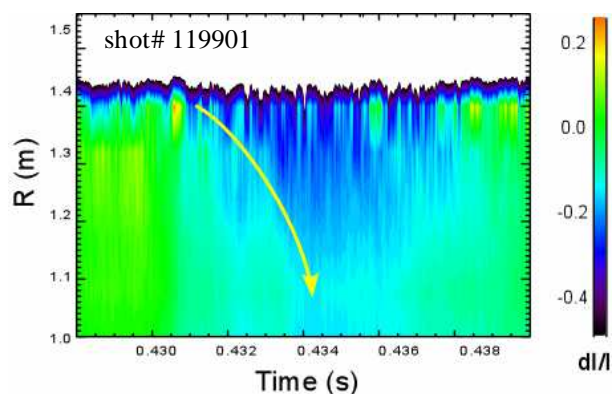


Fig. 4: Relative USXR intensity showing cold pulse following small Type I ELM

~ 4 ms. The calculated χ_e^{pert} results in 10-20 m^2/s over the bulk of the plasma profile, with a correspondingly lower energy loss, $\Delta W_{tot}/W_{tot} \sim 3\text{-}5\%$.

Finally, there have been scans varying the neutral beam heating power which have resulted in discharges with “moderate” size Type I ELMs resulting in $\Delta W_{tot}/W_{tot} \sim 10\%$. The ELM perturbation behavior of

these discharges is similar to that of the DND plasma with smaller Type I ELMs, though the timescale of the cold pulse propagation to the plasma core is faster, ~ 2 ms, with a calculated $\chi_e^{pert} \sim 30\text{-}50 \text{ m}^2/\text{s}$ over the bulk of the plasma. Thus, there appears to be a direct correlation between the calculated perturbed electron thermal transport and the corresponding energy loss

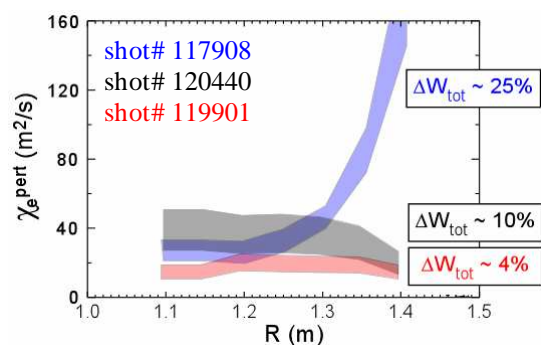


Fig. 5: Calculated χ_e^{pert} for large, medium, and small Type I ELMs

over the range of these ELMs (Fig. 5). Given this scaling, the severity of ELMs can be used as an indicator of the underlying perturbed transport properties. This knowledge could in principle be used to optimize the ELM size to provide sufficient impurity exhaust while avoiding large heat pulses to the divertor plasma-facing components.

Work supported by US DoE grant DE-FG02-99ER5452 at JHU

¹R. Maingi, K. Tritz, E.D. Fredrickson, J.E. Menard, et. al., *Nucl. Fusion* 45 (2005) 264.

²R. Maingi, C.E. Bush, E.D. Fredrickson, D.A. Gates et. al., *Nucl. Fusion* 45 (2005) 1066.

³D. Stutman, et. al., *Rev. Sci. Instrum.* 74 (2003) 1982.

⁴M. Soler, J. D. Callen, *Nucl. Fusion* 19, (1979) 703

⁵S. M. Kaye et al., *Nucl. Fusion* 47, (2007) 499